Formation of Colloidal Hydroxy-Sodalite Nanocrystals by the Direct Transformation of Silicalite Nanocrystals

Jianfeng Yao,[†] Huanting Wang,*[,†] Kyle R. Ratinac,[‡] and Simon P. Ringer[‡]

Department of Chemical Engineering, Monash University, Clayton, VIC 3800, Australia, and Australian Key Centre for Microscopy and Microanalysis, The University of Sydney, Sydney, NSW 2006, Australia

Received December 11, 2005
Revised Manuscript Received February 4, 2006

Interest in the synthesis and applications of zeolite nanocrystals has grown continuously since colloidal suspensions of zeolite particles were first reported in the early 1970s.[1] The successful synthesis of zeolite nanocrystals has enabled more advanced studies of the mechanisms of zeolite nucleation and crystal growth. Moreover, the improved performance achieved by using zeolites in the form of nanocrystals has affected their traditional application in areas such as catalysis, ion exchange, adsorption, and separation.[1−4] Perhaps more importantly, nanocrystals have allowed zeolites to find new applications such as as low-*k* dielectrics in microelectronics,[5,6] in chemical sensing,[7,8] and as nanostructured membranes in fuel cells.[9]

Synthesis of colloidal zeolite nanocrystals generally requires the use of a large amount of organic structure directing agent (SDA) to control the process of zeolite crystallization. In the absence of SDA, controlled synthesis of zeolite nanocrystals becomes far more difficult. More recently, workers have developed SDA-free synthesis of zeolite nanocrystals through the use of space-confining additives such as carbon black,[10] starch,[11] gelling polymer,[12,13] and even carbon nanotubes;[14] however, the rational control of the zeolite nanocrystals with a narrow size distribution still remains challenging.[1]

Here we report our findings that colloidal hydroxy-sodalite nanocrystals, free from SDA, can be obtained by the transformation of silicalite nanocrystals. We have used silicalite nanocrystals as the silica source for this process because the synthesis of silicalite is well-established[15,16] and because silicalite nanoparticles made with tetrapropylammonium hydroxide (TPAOH) as a template have a high resistance against dissolution in alkaline solution. Indeed, this has led to their application in corrosion-resistant coatings.[17] After the incorporation of sodium and aluminum and the transformation of the silicalite crystal structure, the resulting hydroxy-sodalite nanocrystals possess sizes and morphologies similar to those of the original nanocrystals.

Sodalite has a framework structure consisting of a six-membered ring aperture with a pore size of 2.8 Å. In particular, the sodalite whose framework charges are balanced with hydroxide anions is termed hydroxy-sodalite. Because of its small pore size and high ion exchange capacity, sodalite is very attractive as a functional material for a wide range of applications such as optical materials,[18−20] waste management,[21,22] hydrogen storage,[23] and hydrogen separation.[24,25] Microsized sodalite crystals can be easily grown with different precursor materials; for example, polycrystalline sodalite particles (500 nm) were produced by solid−solid-phase transformation of pillared clay.[26−28] To date, sols of colloidal hydroxy-sodalite nanocrystals have only been synthesized by homogeneous nucleation in the presence of tetramethylammonium hydroxide.[29] To the best of our knowledge, we have synthesized colloidal, SDA-free hydroxy-sodalite nanocrystals for the first time.

To begin the process, colloidal silicalite nanocrystals were prepared by hydrothermal treatment of a clear solution of tetraethyl orthosilicate and TPAOH.[30] The resulting colloidal

* To whom correspondence should be addressed. Tel.: +61 3 9905 3449. Fax: +61 3 9905 5686. E-mail: huanting.wang@eng.monash.edu.au.
[†] Monash University.
[‡] The University of Sydney.

(1) Tosheva, L.; Valtchev, V. P. *Chem. Mater.* **2005**, *17*, 2494.
(2) Wang, H. T.; Huang, L. M.; Holmberg, B. A.; Yan, Y. S. *Chem. Commun.* **2002**, 1708.
(3) Wang, H. T.; Holmberg, B. A.; Yan, Y. S. *J. Mater. Chem.* **2002**, *12*, 3640.
(4) Lai, Z. P.; Tsapatsis, M.; Nicolich, J. R. *Adv. Funct. Mater.* **2004**, *14*, 716.
(5) Wang, Z. B.; Mitra, A.; Wang, H. T.; Huang, L. M.; Yan, Y. S. *Adv. Mater.* **2001**, *13*, 1463.
(6) Wang, Z. B.; Wang, H. T.; Mitra, A.; Huang, L. M.; Yan, Y. S. *Adv. Mater.* **2001**, *13*, 746.
(7) Mintova, S.; Mo, S. Y.; Bein, T. *Chem. Mater.* **2001**, *13*, 901.
(8) Wang, Z.; Larsson, M. L.; Grahn, M.; Holmgren, A.; Hedlund, J. *Chem. Commun.* **2004**, *24*, 2888.
(9) Holmberg, B. A.; Hwang, S. J.; Davis, M. E.; Yan, Y. S. *Microporous Mesoporous Mater.* **2005**, *80*, 347.
(10) Madsen, C.; Jacobsen, C. J. H. *Chem. Commun.* **1999**, 673.
(11) Wang, B.; Ma, H. Z.; Shi, Q. Z. *Chin. Chem. Lett.* **2002**, *13*, 385.
(12) Wang, H. T.; Holmberg, B. A.; Yan, Y. S. *J. Am. Chem. Soc.* **2003**, *125*, 9928.
(13) Yao, J. F.; Wang, H. T.; Ringer, S. P.; Chan, K. Y.; Zhang, L. X.; Xu, N. P. *Microporous Mesoporous Mater.* **2005**, *85*, 267.
(14) Pham-Huu, C.; Winé, G.; Tessonnier, J. P.; Ledoux, M. J.; Rigolet, S.; Marichal, C. *Carbon* **2004**, *42*, 1941.
(15) Schoeman, B. J.; Sterte, J.; Otterstedt, J. E. *Zeolites* **1994**, *14*, 110.
(16) Hsu, C. Y.; Chiang, A. S. T.; Selvin, R.; Thompson, R. W. *J. Phys. Chem. B* **2005**, *109*, 18804.
(17) Mitra, A.; Wang, Z. B.; Cao, T. G.; Wang, H. T.; Huang, L. M.; Yan, Y. S. *J. Electrochem. Soc.* **2002**, *149*, B472.
(18) Brenchley, M. E.; Weller, M. T. *J. Mater. Chem.* **1992**, *2*, 1003.
(19) Acar, A. C.; Yücel, H.; Çulfaz, A. *Chem. Eng. Commun.* **2003**, *190*, 861.
(20) Arieli, D.; Vaughan, D. E. W.; Goldfarb, D. *J. Am. Chem. Soc.* **2004**, *126*, 5776.
(21) Buhl, J. C.; Gesing, T. M.; Kerkamm, L.; Gurris, C. *Microporous Mesoporous Mater.* **2003**, *65*, 145.
(22) Oji, L. N.; Williams, A. L. *Nucl. Technol.* **2004**, *145*, 215.
(23) Buhl J. C.; Gesing, T. M.; Rüscher, C. H. *Microporous Mesoporous Mater.* **2005**, *80*, 57.
(24) Julbe, A.; Motuzas, J.; Cazevielle, F.; Volle, G.; Guizard, C. *Sep. Purif. Technol.* **2003**, *32*, 139.
(25) Xu, X. C.; Bao, Y.; Song, C. S.; Yang, W. S.; Liu, J.; Lin, L. W. *Microporous Mesoporous Mater.* **2004**, *75*, 173.
(26) Lee, S. R.; Han, Y. S.; Park, M.; Park, G. S.; Choy, J. H. *Chem. Mater.* **2003**, *15*, 4841.
(27) Choy, J. H.; Lee, S. R.; Han, Y. S.; Park, M.; Park, G. S. *Chem. Commun.* **2003**, 1922.
(28) Lee, S. R.; Park, M.; Han, Y. S.; Choy, J. H. *J. Phys. Chem. Solids* **2004**, *65*, 421.
(29) Schoeman, B. J.; Sterte, J.; Otterstedt, J. E. *Zeolites* **1994**, *14*, 208.
(30) Huang, L. M.; Wang, Z. B.; Sun, J. Y.; Miao, L.; Li, Q. Z.; Yan, Y. S.; Zhao, D. Y. *J. Am. Chem. Soc.* **2000**, *122*, 3530.

10.1021/cm052731+ CCC: $33.50
Published on Web 02/17/2006

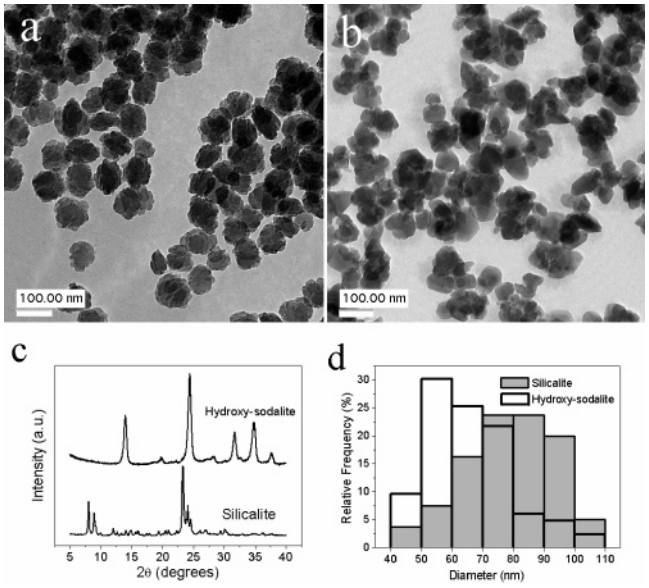

Figure 1. TEM images, XRD patterns, and particle size distributions (PSDs) of nanocrystals. (a) TEM, silicalite; (b) TEM, hydroxy-sodalite; (c) XRD; and (d) PSDs.

silicalite suspension was directly dried at 90−100 °C (see Supporting Information), and these dried nanocrystals were then added into an alkaline solution with a molar composition of 6.07:1:66 $Na_2O/Al_2O_3/H_2O$, which was formed by dissolving sodium hydroxide and sodium aluminate in water. Aging and hydrothermal treatment of this suspension resulted in the conversion of the silicalite nanocrystals into sodalite nanocrystals. After washing and drying, we characterized the precursor silicalite nanocrystals and the final sodalite nanocrystals by transmission electron microscopy (TEM) and X-ray diffraction (XRD). The TEM images shown in Figure 1 indicate that both the silicalite nanocrystals (denoted Sil-N) and sodalite nanocrystals (denoted Sod-N) exhibit similar, compact crystal morphologies with sizes ranging from 40 to 110 nm (Figure 1a,b,d). The average crystal size decreases from approximately 80 nm for Sil-N to 60 nm for Sod-N. The XRD patterns confirm that both types of particles are highly crystalline (Figure 1c). Additionally, the sodalite nanocrystals can be readily dispersed in water or ethanol under mild ultrasonication, and the colloidal sodalite suspensions thus formed are stable for weeks.

To help understand the phase transformation mechanism of silicalite nanocrystals to sodalite nanocrystals, we carried out thermogravimetric analysis (TGA) on the silicalite samples and on the dispersible sodalite nanocrystals (Sod-N); the results are shown in Figure 2. The mass lost by the pure hydroxy-sodalite was approximately 10% owing to the removal of structural water (Figure 2c). On heating to 120 °C, the dried pure silicalite lost 2.5% of its mass because of desorption of adsorbed water (Figure 2b). The further 13.5% mass loss above 120 °C is close to the 11.7% loss calculated assuming four TPA^+ cations per unit cell in a pure silicalite crystal; therefore, we attribute this mass loss to the decomposition of occluded TPAOH molecules in the silicalite structure. The directly dried silicalite nanocrystals showed a total mass loss of 29% (Figure 2a).

After allowing for the 16% lost by the dried pure sample, the remaining decrease in mass must be due to approximately

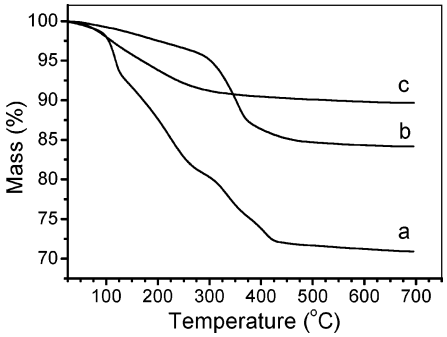

Figure 2. TGA curves of (a) directly dried as-synthesized silicalite nanocrystals, (b) dried pure silicalite nanocrystals, and (c) hydroxy-sodalite nanocrystals.

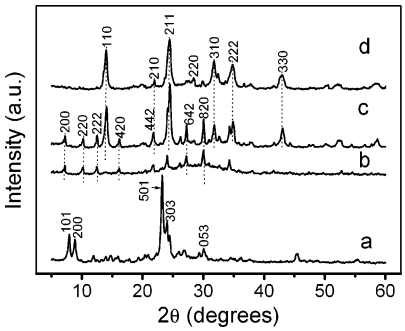

Figure 3. XRD patterns of samples prepared with directly dried silicalite nanocrystals by hydrothermal treatment at 80 °C for (a) 0, (b) 1, (c) 2, and (d) 3 h. Prior to heating, all the samples were aged at room temperature for 4 h.

13% of additional TPAOH associated with the directly dried silicalite nanocrystals. The extra TPAOH molecules in excess of those in the zeolitic channels should reside in the intercrystal pores, that is, in the packing pores and on the surfaces of the silicalite nanocrystals.[31,32] These surface molecules should serve as a barrier that isolates the silicalite nanocrystals during the attack of the alkaline solution, preventing the nanocrystals from agglomerating. We believe that this barrier plays a crucial role in the formation of dispersible sodalite nanocrystals, explaining the coarsening of the sodalite nanocrystal morphologies obtained when dried pure silicalite is used in place of directly dried silicalite (Sil-N).

To further clarify the transformation process of silicalite nanocrystals, we aged the directly dried silicalite nanocrystals in alkaline solution at room temperature and then hydrothermally treated them at 80 °C for different times. Comparison of the XRD pattern in Figure 3a with that for Sil-N in Figure 1c reveals that the peak intensities (units not shown) of the silicalite nanocrystals remain almost unchanged after 4 h aging; this confirms the stability of the silicalite nanocrystals in alkaline solution at room temperature. Considering the other data in Figure 3, it is evident that the silicalite was mostly transformed to zeolite A after only 1 h of heating. A mixture of zeolite A and sodalite was observed after 2 h of heating (Figure 3c); pure sodalite was obtained with 3 h of heating.

Fourier transform infrared (FT-IR) spectra (Figure 4) show the samples transforming from silicalite to sodalite. With

(31) Wang, H. T.; Wang, Z. B.; Huang, L. M.; Mitra, A.; Holmberg, B.; Yan, Y. S. *J. Mater. Chem.* **2001**, *11*, 2307.
(32) Wang, H. T.; Wang, Z. B.; Yan, Y. S. *Chem. Commun.* **2000**, 2333.

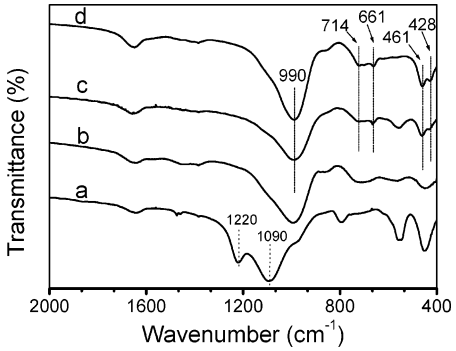

Figure 4. FT-IR spectra of samples prepared by heating at 80 °C for different periods of time: (a) 0, (b) 1, (c) 2, and (d) 3 h.

increasing heating time, the characteristic bands of the silicalite Si−O−Si framework, such as the double-ring vibration at approximately 550 cm^{-1} and the stretching vibrations at 1090 and 1220 cm^{-1}, gradually disappear; instead, the characteristic adsorption band at 428 cm^{-1} appears as the single four-membered ring (S4R) of the sodalite unit is formed.[28] In the IR spectrum of the pure sodalite sample (Figure 4d), the broad band at approximately 990 cm^{-1} is assigned to the asymmetric stretch (T—O—T, T = Si, Al), the adsorptions between 714 and 661 cm^{-1} are due to the symmetric stretch (T—O—T), and the bands at 461 and 428 cm^{-1} arise from the bending vibration of O—T—O.[33,34]

Energy-dispersive X-ray spectroscopy (EDXS) could not detect sodium or aluminum in the aged sample, again indicating that the silicalite nanocrystals were stable in alkaline solution at room temperature. However, when the dispersion of silicalite in alkaline solution was heat-treated at 80 °C, both sodium and aluminum ions rapidly entered the silicalite framework; this was evidenced by the change in the molar ratio of Na/Si/Al from 0:1.00:0 at 0 h to 1.21:1.27:1.00 after 1 h to 1.30:1.10:1.00 after 2 h, finally reaching 1.44:1.02:1 after 3 h. Despite the limitations of EDXS in quantifying the sodium content accurately, the trend of the change in sodium content should be reliable. Elemental analysis (Galbraith Laboratories, TN) confirms that the pure hydroxy-sodalite nanocrystals obtained in this work have a molar Na/Si/Al ratio of 0.99:1.06:1.00, in good agreement with the standard composition of hydroxy-sodalite.

On the basis of the foregoing experimental results, the transformation of silicalite nanocrystals into hydroxy-sodalite nanocrystals is illustrated schematically in Figure 5. The as-synthesized colloidal silicalite nanocrystals are directly dried so that the excess TPAOH molecules and any small amounts of silica species coat the nanocrystals.[31] The directly dried silicalite nanocrystals retain the MFI structure when they are in contact with the alkaline solution at room temperature. During subsequent heating, the alkaline solution attacks the silicalite structure, allowing sodium and aluminum ions enter the lattice; meanwhile, the TPA^+ ions in the silicalite zeolitic channels are driven out of the nanocrystal frameworks by exchange with the high concentration of Na^+ ions. During

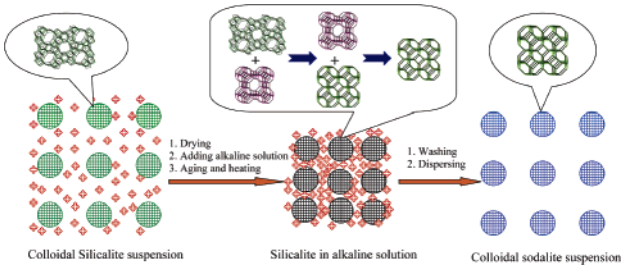

Figure 5. Schematic representation of the phase transformation of silicalite nanocrystals into sodalite nanocrystals.

this process, the crystal structure evolves in the following stages:

silicalite (MFI) ⟹ silicalite (MFI) + zeolite A (LTA) ⟹ zeolite A (LTA) + hydroxy-sodalite (SOD) ⟹ hydroxy-sodalite (SOD)

The resultant hydroxy-sodalite nanocrystals possess a smaller average size as compared with the starting silicalite nanocrystals (Figure 1d). This is at least partially because the pore volume of hydroxy-sodalite (SOD) is smaller than that of silicalite (MFI), which causes the nanocrystal frameworks to shrink during the phase transformation and leads to smaller particles. In addition, because of their small size, it seems likely that the silicalite nanocrystals partially dissolved into the alkaline solution during heating. The hydroxy-sodalite nanocrystals formed by this process can be easily dispersed by washing away the temporary barrier of TPAOH and then re-dispersion in solvents such as water or ethanol. Given their size, the TPAOH molecules in this system do not function as templates for the hydroxy-sodalite structure; they appear solely to constrain crystal growth and prevent agglomeration of the nanocrystals during the reaction.

In summary, colloidal, SDA-free hydroxy-sodalite nanocrystals have been successfully synthesized by the transformation of silicalite nanocrystals. The morphologies and sizes of the hydroxy-sodalite nanocrystals obtained are similar to those of the starting silicalite nanocrystals. It should be possible to synthesize other types of colloidal aluminosilicate nanocrystals, such as zeolites A, X, or Y, by carefully altering the transformation conditions such as the composition of the alkaline solution and the reaction temperature. Importantly, this work has also provided a new insight into the nucleation and growth of zeolite nanocrystals. We expect the SDA-free hydroxy-soldalite nanocrystals to be useful for fabricating nanostructured porous materials and nanocomposite membranes.

Acknowledgment. This work was supported by the Australian Research Council (Discovery Project No. DP0559724) and Monash University. The facilities and technical assistance from staff at Electron Microscopy and Microanalysis Facility, Monash University, are gratefully appreciated. H.W. thanks the Australian Research Council for the QEII Fellowship.

Supporting Information Available: Experimental section and the effect of the pretreatment of silicalite nanocrystals (PDF). This material is available free of charge via the Internet at http://pubs.acs.org.

CM052731+

(33) Johnson, G. M.; Weller, M. T. *Stud. Surf. Sci. Catal.* **1997**, *105*, 269.
(34) Hasha, D.; de Saldarriaga L. S.; Saldarriaga, C.; Hathaway, P. E.; Cox, D. F.; Davis, M. E. *J. Am. Chem. Soc.* **1988**, *110*, 2127.